IJST, Transactions of Civil Engineering, Vol. 36, No. C2, pp 225-238
Printed in The Islamic Republic of Iran, 2012

EVALUATION OF CLIMATE CHANGE IMPACT ON REGIONAL FLOOD CHARACTERISTICS*

M. KARAMOUZ[1],** M. FALLAHI[2] AND S. NAZIF[3]

[1]Polytechnic Institute of NYU, Brooklyn, NY, School of Civil Engineering, University of Tehran, Tehran, I. R of Iran
Email: Karamouz@ut.ac.ir
[2]School of Civil Eng, Amirkabir University of Technology, Tehran, Iran, I. R of Iran
[3]School of Civil Engineering, University of Tehran, Tehran, I. R of Iran

Abstract– Floods are one of the most important natural disasters causing extensive loss of life and properties every year all over the world. Occasional tropical or Mansoon rain can produce floods that are sometimes considered as a lifesaver due to water scarcity in arid and semi-arid regions. By simulating the hydrograph of probable floods in each year, action plans can be implemented to reduce damages and also to better plan for utilizing water resources potential of floods. By simulating future rainfall, and estimating the resulted runoff, it can be determined whether a severe flood will occur or not. The simulated flood hydrograph is affected by uncertainties in future rainfall simulation and runoff modeling that should be considered when flood prevention plans are developed. In this study, a long lead flood simulation model is developed, considering the uncertainties in the simulation process. The SDSM (Statistical Downscaling Model) is used to generate hourly and daily rainfall data, needed for flood simulation, based on General Circulation Models (GCM) outputs. The extreme simulated rainfalls in each year are considered as the probable flood and a rainfall-runoff model developed in HEC-HMS software environment is used for simulation of the corresponding hydrograph. The uncertainties in hydrograph development are considered through variation of curve number (CN) and time of concentration (T_c). The effect of climate change on flooding probability is evaluated by comparing the Cumulative Distribution Function (CDF) of the simulated floods with historical floods. The proposed model for long lead flood simulation has been applied to the Kajoo basin located in the south-eastern part of Iran.

Keywords– Uncertainty, long lead flood simulation, downscaling, rainfall-runoff model

1. INTRODUCTION

Long lead flood simulation is an effective tool in flood damage prevention/reduction using optimization schemes as Karamouz et al. [1]. Long lead flood simulation process is affected by many parameters with considerable uncertainties. Global climate change will have a significant impact on the mid to long-term planning for prevention of flood damages by simulating their special characteristics such as flood frequencies and magnitudes in local and regional hydrologic systems. In addition to water resource planners who are required to include the likely impacts of climate change on current water policies and capital investment plans, especially in the flood fields, do so against a background of considerable uncertainty [2]. Many of these uncertainties arise from the stochastic nature of global climate as a physical system. The uncertainties in runoff simulation, especially floods, are mainly due to 2 types of uncertainties. The first is future rainfall simulation uncertainty and the 2nd is uncertainty due to rainfall-runoff model parameters. An important step in looking for causes of flood is to understand the source of uncertainty related to performance assessment of drainage systems. Hansen et al. [3] introduced a

*Received by the editors January 14, 2010; Accepted October 9, 2011.
**Corresponding author

methodology for design and analysis of urban drainage systems that takes into account the uncertainties related to the model inputs and parameters. For less complex situations, the first order analysis of uncertainty is used, while the Monte Carlo method is also used for more elaborate situations. In both cases, the uncertainty analysis leads to reliability based design of urban drainage systems, which can be setup for any desired confidence level. Jiang et al. [4] investigated potential impacts of human-induced climate change on the water availability in the Dongjiang basin, South China, using six monthly water balance models. The capability of the six models in simulating the present climate water balance components is first evaluated, and the results of the models in simulating the impact of the supposed climate change are then analyzed and compared. The results of the analysis reveal that all six conceptual models have similar capabilities in reproducing historical water balance components. Greater differences in the model results occur when the models are used to simulate the hydrological impact of the proposed climate changes. The study provides insights into the considered changes in the basin's hydrology due to climate change, that is, it shows that there can be significant implications for the investigation of response strategies for water supply and flood control scenarios due to climate change. Burger et al. [5] presented kernel-based learning machine river flow models for the Upper Gallego catchment of the Ebro basin. The models posed two major challenges: (1) estimation of the rainfall-runoff transfer function from the available time series is complicated by anthropogenic regulation and mountainous terrain and (2) the river flow model is weak when only climate data are used, but additional antecedent flow data seemed to lead to delayed peak flow estimation. These types of models, together with the presented downscaled climate scenarios, can be used for climate change impact assessment. Krysanova et al. [6] studied the implications of complexity and uncertainty in climate change impact assessment at the river basin and regional scales. The study was performed using the process-based ecohydrological spatially semi distributed model SWIM (Soil and Water Integrated Model). The model integrates hydrological processes, vegetation/crop growth, erosion and nutrient dynamics in river basins. It was developed from the SWAT and MATSALU models for climate and land use change impact assessment. The study area is the German part of the Elbe River basin (about 100,000 km^2). The uncertainty of climate impacts was evaluated using comprehensive Monte Carlo simulation experiments. Day [7] utilized the ESP (Ensemble Stream flow Prediction) model for runoff prediction. In their approach, a hydrological model using current in stream flow, rain and temperature time series is developed which calculates the probable flow hydrographs. Then a statistical model that determines the statistical distribution of rainfall in future time periods is implemented. Ingram et al. [8] investigated an advanced method for hydrological prediction in real time. The most important characteristic of their system was the real time prediction by using the meteorological predictions. Azmi et al. [9] used five different models of data fusion for streamflow forecasting. The results show the capability of the combined models in streamflow forecasting.

Harpham and Wilby [10] simulated the precipitation for different parts of England using various models such as SDSM, radial neural network and multi layers neural network. The results of their investigation show that all of these methods are capable of simulating precipitation; however, in different zones their capabilities are different. Ekstorm et al. [11] assessed the effects of selecting the probability distributions of rainfall and temperature variables on the runoff distribution. The results show that different probability functions for rainfall and temperature can affect the flow distribution function. In this paper, a methodology for long-lead flood simulation has been developed using downscaled rainfall data. Sensitivity analysis has been done on the results by considering uncertainties in downscaling procedure and parameters estimation of the rainfall- runoff model. This section is followed by an introduction to the study area characteristics and the data resources. Then the future rainfall simulation and downscaling procedure is described. In the following section a description of a rainfall- runoff model and its calibration

is given. In the results section, uncertainty analysis of the future rainfall and flood simulation and the rainfall- runoff model parameters as well as future trends of flood are presented. Finally, a summary and conclusion are given.

2. STUDY AREA

The study area is the Zirdan dam sub basin at the Kajoo River basin with an area of 3659 km^2, in the South Baloochestan region located in the south-eastern part of Iran. Because of the limited flood carrying capacity of the Kajoo River, yearly floods cause damages to the agricultural lands and the rural areas. Therefore, future flood simulation in this area is vital for development of warning schemes and contingency plans for flood damage prevention. The study area includes 12 sub-basins identified based on physiographic studies; the physical characteristics and the placement of each of these sub-basins are presented in Table 1 and Fig. 1, respectively. In the past fifteen years, six considerable floods have occurred in the years of 1991,1992,1995,1997 and 2005 in this region. These floods left behind extensive damages that show the vulnerability of the study area to floods and the significance of future flood simulation with adequate lead time. The rainfall data at the Ghasre-Ghand station, which is the only available meteorological station inside the Zirdan dam sub-basin, is used for developing rainfall simulations and downscaling model. Twenty four years (1976–1999) of daily rainfall data has been used in this station which is used as predictands. Based on WMO recommendations the basic normal window for climate models results calibration and verification is considered to be 30 years, however in this study only 24 years of data is available and used for models development. This could be a shortcoming in climatic studies and has to be extended once additional data is obtained/collected.

Table 1. The characteristics of sub-basins in the study area

Sub-basin	A (km^2)	L (km)	T_C(mean) (hr)	T_C (Bransby& Williams)	T_C (Kirpich)
1	535	28	5.46	7.43	3.48
2	175	10	1.66	2.3	1.01
3	422	21	3.76	5.17	2.34
4	66	13	2.66	3.75	1.56
5	317	38	2.39	3.29	1.49
6	450	39	7.21	10.16	4.26
7	395	39	8.28	11.43	5.12
8	506	32	5.73	8.01	3.46
9	50	13	2.82	4.04	1.61
10	73.3	13	2.83	3.91	1.75
11	255	25	5.13	7.08	3.18
12	295	18	3.17	4.44	1.9

The historical rainfall data shows that devastating floods occur in the winter (January to March). Furthermore, the only measured flood hydrograph that is officially released and used for calibration has occurred in winter. Therefore, to develop the methodology and test it, winter rainfalls/floods are considered. Observed large-scale NCEP (National Centre for Environmental Prediction) reanalysis atmospheric variables for the same period (for 60-63.75E, 25-27.5N) have been used as predictors. Also, hydrographs of observed historical floods at the Ghasre-Ghand station during the study period have been gathered for rainfall-runoff model calibration.

Fig. 1. The study area of Kajoo River basin

3. RAINFALL DOWNSCALING

The downscaling model used in this study is a multiple regression based model and is referred to as Statistical Down-Scaling Model (SDSM). The analytical base of this model is formulated by Wilby et al. [10]. In downscaling with the SDSM, a multiple linear regression model is developed among few selected large-scale predictors and the local scale predictands such as rainfall. The model has been organized in two steps for rainfall downscaling. In the first step, it is determined each day whether rainfall occurs or not, as follows:

$$\omega_i = \alpha_0 + \sum_{j=1}^{n} \alpha_j \hat{u}_i^{(j)} \tag{1}$$

where ω_i is the conditional probability of rainfall occurrence on day i, $\hat{u}_i^{(j)}$ is the normalized amount of predictor j on day i and α_j is the estimated regression coefficient. Rainfall in day i occurs if $\omega_i \le r_i$, where r_i is a stochastic output from a linear random- number generator. Value of rainfall in each rainy day is estimated in the second step using Z score as follows:

$$Z_i = \beta_0 + \sum_{j=1}^{n} \beta_j \hat{u}_i^{(j)} + \varepsilon \tag{2}$$

$$Z_i = \phi^{-1}[F(y_i)] \tag{3}$$

where Z_i is the z-score calculated by the estimated regression equation with coefficient β_j for predictor j, and the normally distributed stochastic error term ε. Then the rainfall value, y_i, in Equation 3 is calculated from the cumulative distribution function ϕ of the empirical distribution function $F(y_i)$ of the daily rainfall occurrence. It must be noted that the same predictors in the standardized form are used to model rainfall occurrence and depth. The correlations between different combinations of available climatic predictors and daily rainfall data have been calculated to find the most appropriate predictors of rainfall in the study area. It must be noted that only the winter (January, February, and March) rainfall has been considered for this purpose because it constitutes about 75% of the annual rainfall and all major floods occur in these months. A combination of predictors has been selected for long lead rainfall simulation because of their maximum correlation with daily rainfall. Correlation coefficients between selected predictors and daily rainfall have been presented in Table 2. This table also reports the P-value between the predictors and rainfall that help to identify the amount of explanatory power for each predictor. P-value is a statistical parameter that measures the probability of accidental high correlation between predictands and predictors numerically. If P-value is small, the correlation is more realistic. As the distribution of daily rainfall is skewed, a fourth root transformation is applied to the original series to convert it into a normal distribution, and then it is used in regression analysis; Fig. 2 shows this transformation. The model is structured in monthly time scale for rainfall downscaling, in which twelve regression equations are derived for twelve months. The model is calibrated and validated using 15 years (1976–1990) and 9 years (1991–1999) of daily data of observed predictors and predictands respectively, and one hundred ensembles of downscaled daily rainfall have been generated. Table 3 also shows the errors of maximum and mean downscaled rainfall data. Through the above procedure, the weather generator is used to downscale observed (NCEP) predictors, and generate scenarios to downscale the considered scenarios for future climate variation. HadCM3 (Second Hadley Centre Coupled Ocean-Atmosphere GCM) scenario A2 and B2 data which is available from year 2000 to 2099, is used as a model input signal and one hundred ensembles of downscaled daily rainfall have been generated. In these scenarios, green house gas emissions and economic and social development effects on the future climate are considered. The A2 scenario describes a completely different condition of the world. The underlying theme is self reliance and preservation of local identities and the population will grow continuously. However, in this scenario per capita economic growth and technological change are slower than other scenarios. In the B2 scenario emphasis is on local solutions to achieve economic, social and environmental sustainability. To ensure the appropriate performance of the downscaling model, regarding the characteristics of the observed data, nonparametric methods are employed to test the equality of mean and variance of the downscaled and observed data. The details of these methods applications are discussed in the following sections.

- ***Wilcoxon signed rank test***

For constructing a hypothesis test p-value for equality of means of observed and downscaled data (difference of two population means), the Wilcoxon signed rank method is used [11]. This is also true about the downscaling procedure followed in this study. A detailed description of the theory of Wilcoxon signed rank test can be found in Conover [12] and Neter et al. [13]. When it can be assumed that the population of differences is symmetrical, the Wilcoxon signed rank test is generally more powerful than the sign test for making inferences about the population median differences (η_D). In practice and especially in experimental settings, the population of differences between matched pairs will frequently be symmetrical, or approximately so. Given the approximate normality of sum the signed ranks and denote the sum (*T*), the construction of the decision rule proceeds as usual for large- sample tests. When the alternatives are:

$$\begin{aligned} H_0 \quad & (null\ hypothesis): \eta_D = 0 \\ H_1 \quad & : \eta_D \neq 0 \end{aligned} \tag{4}$$

the appropriate decision rule to control the α risk in application of the test is calculated as follows:

$$\begin{aligned} & if \quad A_1 \le T \le A_2, \ conclude\ H_0 \\ & if \quad T < A_1 \ or \ T > A_2, \ conclude\ H_1 \\ & where: \\ & A_1 = 0 + z(\alpha/2)\sqrt{\frac{n(n+1)(2n+1)}{6}} \\ & A_2 = 0 + z(1-\alpha/2)\sqrt{\frac{n(n+1)(2n+1)}{6}} \end{aligned} \tag{5}$$

where *z(j)* is the *100(j)* percentile of the standard normal distribution and n is the sample size. MATLAB 7.0 software is used to perform this test. The results of this test application are given in Table 4. As can be seen, the results are all meaningful in 95% confidence level.

Table 2. The Results of selected predictors for rainfall prediction in the study area

Predictor	Correlation coefficient between weather –variables and rainfall	P_v (P value)	Pr (Partial correlation)
relative humidity at 850 hPa altitude	0.42	0.002	0.48
Near surface specific humidity	0.45	0.000	0.5
Near Surface relative humidity	0.40	0.000	0.44

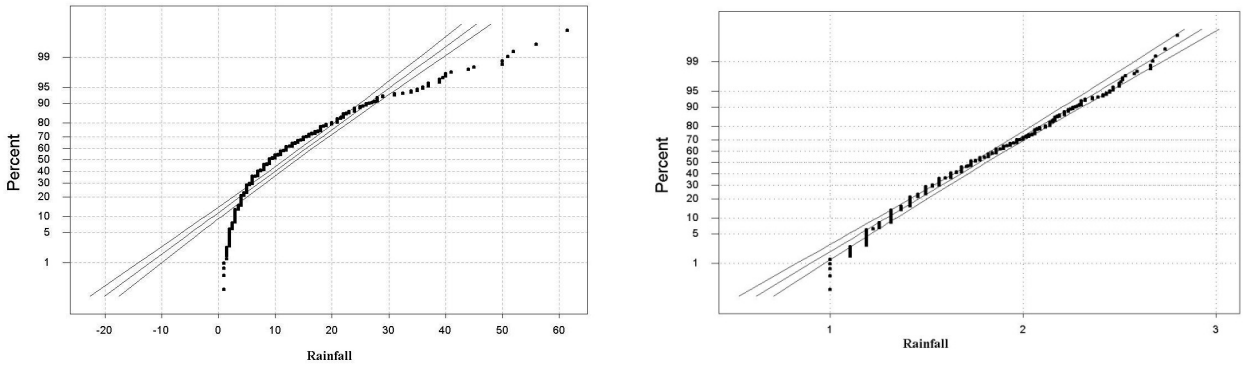

Fig. 2. Fourth root transformation to the original rainfall series

Table 3. The errors between simulated and observed rainfall for (1991-1999)

MAE	Mean	Maximum
Simulated rainfall by (H3A2a) scenario (mm)	2.8	5
RMSE		
Simulated rainfall by (H3A2a) scenario (mm)	2.8	7

Table 4. The results of performing Wilcoxon rank sum tests for evaluation of simulated of rainfall

Parameter	GCM Model	(Variance)		(Mean)
		Leven's test		Wilcoxon rank sum test
		p-value	Test Statistic	p-value
Rainfall	NCEP	0. 995	0.0001	0.977
	HAD (A)	0.827	0.049	0.665
	HAD (B)	0.963	0.002	0.5636

- ***Modified Levene's test***

Modified Levene's test suggested by Brown and Forsythe [14] is used in this study to test the equality of variance of downscaled and observed data. Levene's test is used when the data come from continuous, but not necessarily normal, distributions. In this method the distances of the observations from their sample median are calculated. The Levene test is defined as:

$$\begin{aligned} H_0 &: \quad \sigma_1 = \sigma_2 = ... = \sigma_k \\ H_a &: \quad \sigma_i \neq \sigma_j \text{for at least one pair (i, j)} \end{aligned} \tag{6}$$

Given a variable *Y* with sample of size *N* divided into *k* subgroups, where N_i is the sample size of the *ith* subgroup and σ_i denotes the standard deviation of the *i* subgroup. The Levene test statistic is defined as:

$$w = \frac{(N-k)\sum_{i=1}^{k} N_i (\overline{Z}_{i0} - \overline{Z}_{00})^2}{(k-1)\sum_{i=1}^{k}\sum_{j=1}^{N_i} (Z_{ij} - \overline{Z}_{i0})^2} \tag{7}$$

and

$$Z_{ij} = \left| Y_{ij} - \overline{Y}_{i0} \right| \tag{8}$$

where Y_{ij} is the value of the *j*th sample from the *i*th group, $\overline{Y}_{i0}$ is the mean of all Z_{ij} , $\overline{Z}_{00}$ is the mean of all Z_{ij} and $\overline{Z}_{i0}$ *is* the mean of the Z_{ij} for group *i*, and are calculated as follows:

$$\overline{Z}_{00} = \frac{1}{N}\sum_{i=1}^{k}\sum_{j=1}^{N_i} Z_{ij} \tag{9}$$

$$\overline{Z}_{i0} = \frac{1}{N_i}\sum_{j=1}^{N_i} Z_{ij} \tag{10}$$

MINITAB 13.0 is used for performing Levene's test.The results of the test application are given in Table 4. The results of this test are the same as the Wilcoxon text. In the next step, 100 ensemble data of rainfall have been generated for uncertainty analysis. The results show that there is no meaningful difference between these climate change scenarios, which is why the results of scenario Had A2 are considered in the proceedings of this paper. It should be noted that different GCM models define various climate change scenarios whose analysis could be useful for evaluation of uncertainties. However the data of other models cannot be accessed, and the studies show that scenarios developed by HadCM3 could considerably cover possible future climate changes. In this paper monthly maximum rainfall that have high potential for flood

are considered. Therefore, the simulated and observed mean maximum rainfall in each month during the validation period is compared as shown in Fig. 3. This figure shows the capability of the rainfall simulation model for configuration of monthly maximum rainfall variations. There are some deviations in the observed data, especially in the months of April and June which are not important in this study, because only the winter rainfall has been considered for simulation. For flood simulation, first the rainfalls that cause flood must be identified. For this purpose, the maximum simulated rainfall in each ensemble has been used as rainfall that causes flood. The selected rainfall is imported to rainfall-runoff model for flood simulation. For investigation of compatibility of the simulated and observed rainfall, the CDFs of maximum winter rainfalls are developed for both time series (Fig. 4). The developed CDFs for periods of 1991-99 are compared and the results show the consistency of the downscaling procedure. The probabilities of exceedance of simulated and observed rainfall events are closely matched. This is true with flood events as well. It can be concluded that the flood return periods are magnitudes, which are also preserved.

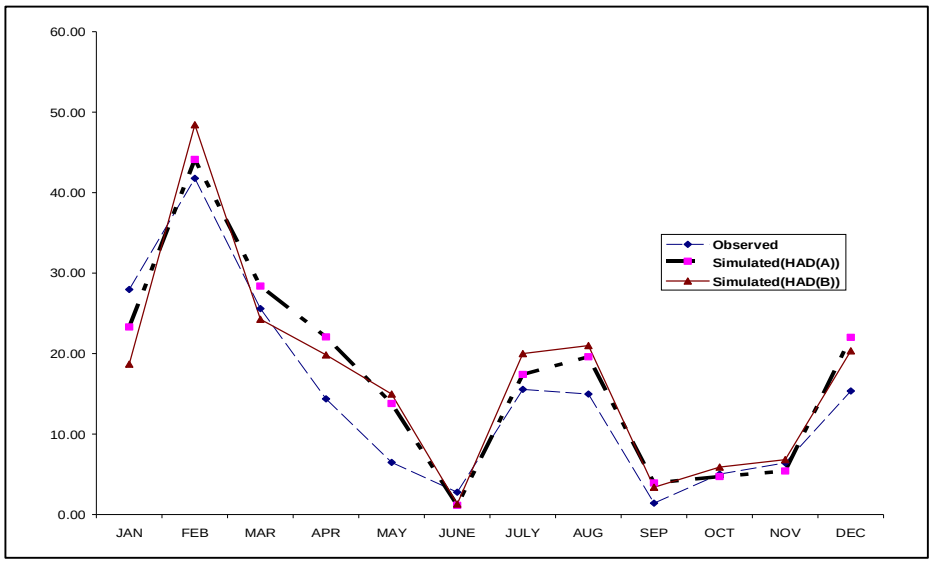

Fig. 3. observed and simulated data at the validation period (1991–1999) (in mm)

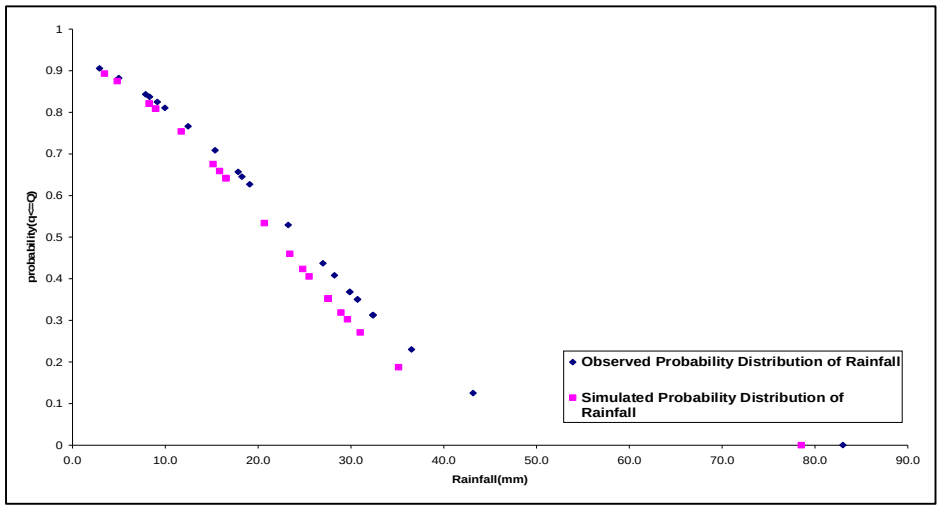

Fig. 4. Simulated and observed probability distribution of rainfall for 1991-1999

4. RAINFALL-RUNOFF MODEL

Karamouz [15] developed a rainfall-runoff model by using HEC-HMS software and the soil conversation service (SCS) method has been used for runoff estimation. The available rainfall data of flood 1991 are converted to the hourly hyetograph that is needed for rainfall-runoff model calibration. This has been done using the central pattern of SCS hyetograph. This pattern has monotonic and steady intensity during the rain, the same as the observed rainfall pattern in the study area. An average CN of 85 for moderate humidity antecedent moisture condition (AMC-II) has been estimated for the basin; see also Karamouz et al. [16]. The calibrated rainfall-runoff model performance in simulating the other floods (occurred in years 90, 91, 96, 98 and 2005) in the study area is also checked. Since the model has well simulated the considered floods it has been employed for further analysis in the study area. The simulated hyetograph for rainfall that caused the February 1991 flood has been used in the HEC- HMS model for model calibration. As a theoretical pattern of rainfall has been used for developing hourly rainfall hydrographs, due to lack of data, only the peak values are compared with the observed floods. There is a difference of 4% between the observed and simulated peak of flood 1991. For other historical floods (1991, 1992, 1995, 1997 and 2005), the same procedure is followed and the peak floods are estimated. The calculated errors are less than 10% in all cases.

5. UNCERTAINTY ANALYSIS

In all fields of natural resources management, decision makers face considerable uncertainties and there are a lot of unknown complexities of natural phenomena. Engineers and system analysts make certain assumptions in modeling to develop uncertain outputs. The two main uncertainty sources are the parameter estimation uncertainties in the simulation model and the intrinsic uncertainty in the input data (natural variability of the streamflow). A probabilistic approach is usually used for dealing with uncertainties, especially in the long lead simulation tasks. Through this approach, decision makers will be able to determine the simulated value with desired probability of occurrence or acceptable risk in exceeding different thresholds.

In this paper, uncertainties of long lead flood simulation in each year are analyzed in two approaches: first, uncertainty analysis of the results of rainfall simulations that are used for future flood simulation and the second, evaluation of uncertainty in simulated floods by a rainfall-runoff model.

Approach-1:

As mentioned before, in future rainfall simulation and downscaling procedure, a set of 100 ensembles of daily data are generated. This daily data is transformed to the power of four to match the original data. The maximum rainfall in the winter of the specified years is obtained from each ensemble. Then, a cumulative probability function is fitted to the 100 maximum selected rainfall from different ensembles in each year for uncertainty analysis. The goodness of this fitted function can be evaluated by the probability of occurrence of the observed rainfall. For a close to symmetrical distribution, the expected value of a distribution falls close to the 50% probability of occurrence (The highest point of Probability Density Function (PDF). Therefore once a PDF is estimated based on the ensemble data, the observed value and the 50% simulated event should be compared. The results of probability function fitted to the selected maximum values based on the Anderson (AD) and Chi- square (χ^2) goodness of fit test are presented in Table 5. According to this table, the lognormal distribution has the minimum AD and χ^2 test value; therefore, it is determined as the probabilistic distribution for the selected maximum rainfall data at the Ghasre-Ghand station (R3 in Fig.1). In Fig. 5, the probability distribution of simulated rainfall and the amount of observed rainfall in February of 1991 have been shown as an example. This figure shows that

the observed rainfall of 25mm for this period falls in about 38% probability of occurrence marks. The expected value of simulated rainfall (50% probability of occurrence) is about 22mm. The expected value of other rainfall probability distributions is also in close proximity of the observed values. This could be an effective tool to test the suitability of the assumed CDF and then used for uncertain simulation.

Table 5. The results of fitting probability functions to rainfall data with 95% significance level

Probability distribution / Statistical test	Normal	Lognormal	Weibull	Extreme value	Exponential
χ^2	0.12	0.056	-----	-----	0.32
AD	2.6	0.43	1.63	7.3	14.7

Approach-2:

In this approach, a cumulative distribution function has been fitted to the simulated flood peaks utilizing the 100 ensemble rainfall data through a rainfall-runoff model. The best fitted CDF for simulated flood is lognormal. As an example, the CDF of the simulated floods in the winter of 1991 has been shown in Fig. 6. Here, we tried the same method used in the case of rainfall. As can be seen, by comparing Figs. 5 and 6, the observed flood is closer to the expected flood value which is in about the 0.43 mark. If the 50% mark has the highest density of occurrence (PDF) and a good simulation probability, distribution should tend towards an expected value close to the observed event, then the flood CDF is more representative of the observed value than the rainfall CDF. For evaluating the effect of the 2nd moment (variance), one could conclude that based on the first moment (expected value) of flood, the CDF could be the simulation of the observed flood estimation with higher accuracy. The probability of occurrence of floods or rainfall in a desired interval around the mean value can be estimated by the Chebyshev equation which states that [17]:

$$P[(m_x - h\sigma_x) \le X \le (m_x + h\sigma_x)] \ge 1 - \frac{1}{h^2} \tag{11}$$

where m_x and σ_x are the mean and the standard division of the fitted empirical probability function of variable *X*. *h* is a coefficient which determines the range of simulated values with a probability of occurrence of more than the right side of inequality. As the amount of σ_x increases, the range of *x* with desired probability increases, so the simulations are less certain. This can be quantified using the coefficient of variation (CV). The average CVs of simulated flood and rainfall distribution are 82 and 50 percent, respectively, which show more certainty in future rainfall simulation compared to flood simulation. This is due to the coupled impact of uncertainty of rainfall and parameter estimation uncertainty that contribute to long lead flood simulation. In the second approach for uncertainty analysis, the effects of uncertainty in the rainfall- runoff model parameters estimation are evaluated. The two important parameters considered are the time of concentration (t_c) and the value of Curve Number (CN), which greatly affect the resulted flood hydrograph. For this purpose, different estimations of basin's t_c that are obtained from different empirical functions (Bransby & Williams and Kirpich) are compared with the mean value of t_c. The empirical methods for calculating t_c are as follows:

1- Kirpich's method:

$$t_c = 0.949\left(\frac{L^3}{H}\right)^{0.385} \tag{12}$$

where t_c is the time of concentration (hr) and L and H are the basin length (km) and the difference between the highest and lowest points of basin (m), respectively.

2- Bransby-Williams method:

$$t_c = \frac{0.96L^{1.2}}{H^{0.2}A^{0.1}} \tag{13}$$

where A is the area of watershed (km^2) and L and H are as before. These equations are selected based on the results of a study by Karamouz [18] on the physiographic analysis of the case study. The mean of t_c from the two methods was also considered. Also, CN variations due to soil class and moisture conditions have been considered. CN for AMC-III and AMC-I soil condition has been estimated as 97 and 70, respectively. The results of using the probability distribution of flood estimation for different rainfall-runoff model parameters are shown in Fig. 7. The probabilities of flood simulations are less affected by the time of concentration. Comparing graphs 2, 3, 4 with the same CN in Fig. 7 shows a relatively small shift in CDF with the mean t_c falling in-between as expected. For the same t_c, graphs 1 and 3, the variation in CN results in a considerable shift in CDF. So the model is more sensitive towards this parameter. Therefore graph 3 with mean t_c and CN of 85 is more representative, providing an expected value (50% CDF) close to the observed flood. This is the same as the CDF used in Fig. 6. As shown, the values of CN = 70 (for dry soil conditions) and CN=97 (for dry soil conditions) with the mean value of t_c, yield to the minimum and maximum future flood simulations, respectively. Figure 7 shows that the shape of probability distribution of runoff simulation depends on the variations of CN and t_c. When CN moves towards higher moisture conditions, the simulated values are more scattered. This difference is more noticeable when probability of occurrence floods around 50%. Sensitivity analyses of flood simulations for different probabilities and parameters, shown in Table 6, are performed. For example, using a CN equal to 70 for wet soil conditions and t_c as the empirically estimated value, the peak of flood with the probability of occurrence of less than 40% is simulated as 490 m^3/s. Each of these simulations can be used by the decision makers for developing flood protection programs when they consider the trade-off between flood damages and flood protection costs. The natural variability of rainfall data has been considered through development of 100 ensembles of rainfall data in each year. Furthermore, the uncertainty in the rainfall-runoff model has been considered by different CNs, and time of concentration values and evaluation of their effects on the resulting runoff.

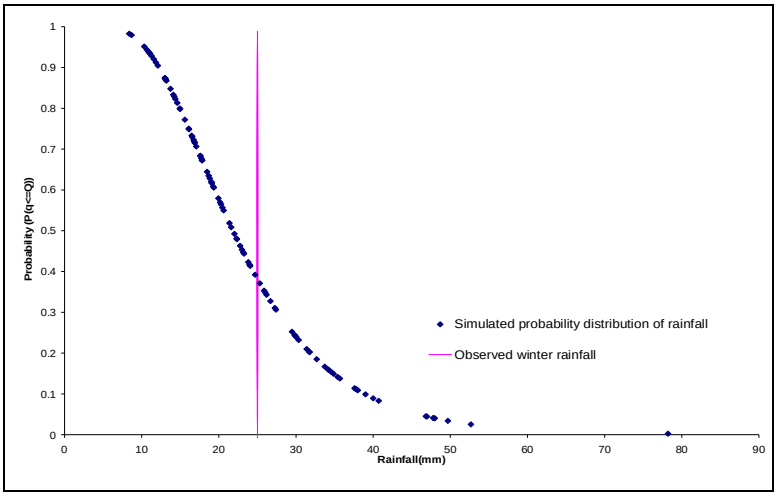

Fig. 5. Simulated probability distribution of rainfall and corresponding value of February 1991

Table 6. Sensitivity analyses of flood predictions to rainfall-runoff models parameters

Case No.	CN	method of estimation of t_c	Peak of flood (m^3/s) (probability of exceeding)				
			20%	40%	50%	60%	80%
1	70	mean value of t_c	795	490	400	323	200
2	85	Bransby&Williamse	1218	786	653	536	342
3	85	mean value of t_c	1515	974	810	664	423
4	85	Kiripich	2051	1293	1072	900	560
5	97	mean value of t_c	3109	2230	1952	1625	1195

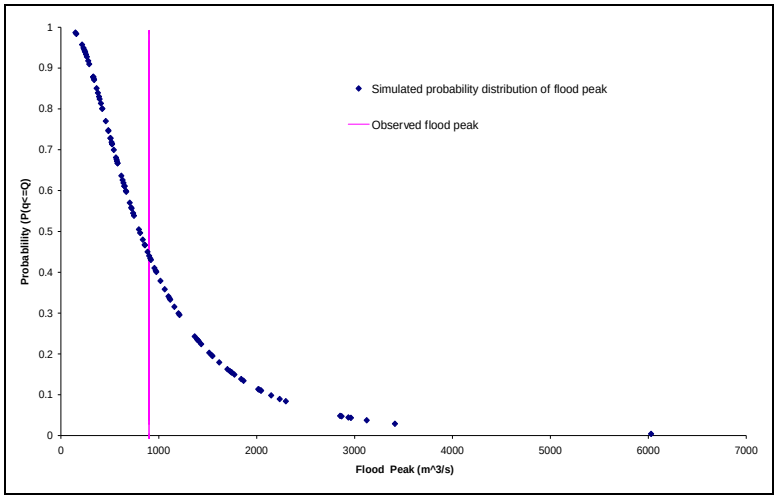

Fig. 6. Simulated probability distribution of flood and corresponding value of February 1991

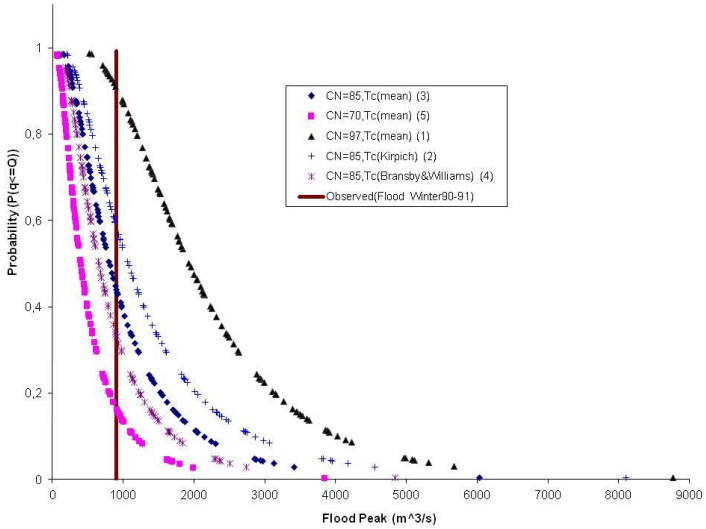

Fig. 7. Risk of flood simulations for year 1991

6. LONG LEAD TRENDS OF FLOOD SIMULATION

For considering the effects of future climate change on the probability of exceedance of flood events, the CDF of simulated rainfall and flood values in periods of 1976-1999, 2000-2020 and 2020-2040 are developed (Figs. 8 and 9). The corresponding probability of exceedances of historical rainfalls and floods in CDF of different periods are compared to evaluate the effect of climate change on hydrological events. The derived simulated rainfall CDF shows that for the low-end rainfall values the probability of exceedances is increasing, but for higher rainfall values the probability of exceedances is decreasing. This is also true for flood events as well. It can be concluded that the severity of the rainfall and flood events in the study region is decreasing under climate change effects.

7. SUMMARY AND CONCLUSION

In this paper, the daily rainfall simulation in the Kajoo river basin located in the South Baloochestan region in Iran, was done using a statistical downscaling model, SDSM. A rainfall-runoff model has been developed to convert the simulated rainfall to runoff in the study area. The rainfall and flood of February 1991 has been used for model calibration. By analyzing the downscaled rainfall data in each year, the rainfall that causes the floods has been characterized and used in the rainfall-runoff model to simulate the

maximum probable peak of flood. The results show that the simulation hydrograph closely matches the observed hydrograph. Uncertainties in future flood simulation have also been studied by two different approaches. In the first approach uncertainties in rainfall simulation have been considered by developing 100 ensembles of data for rainfall and fitting a probability distribution to rainfall. A probability of exceedance could then be selected (i.e. 50%) based on the risk taking attitude of the decision maker and the associated flood could be estimated. The second approach in the analyses of uncertainty in future flood simulation is to evaluate the effects of uncertainty of rainfall-runoff model parameters. For this purpose different values for t_c and CN have been estimated and the probability distribution of flood simulations are developed. The results show that the simulation scheme is more sensitive to CN compared to the time of concentration, t_c. The frequencies of severe flood are decreasing under climate change effects. The results of this study show the significant value of developing tools for contributing uncertainties in long lead flood simulation.

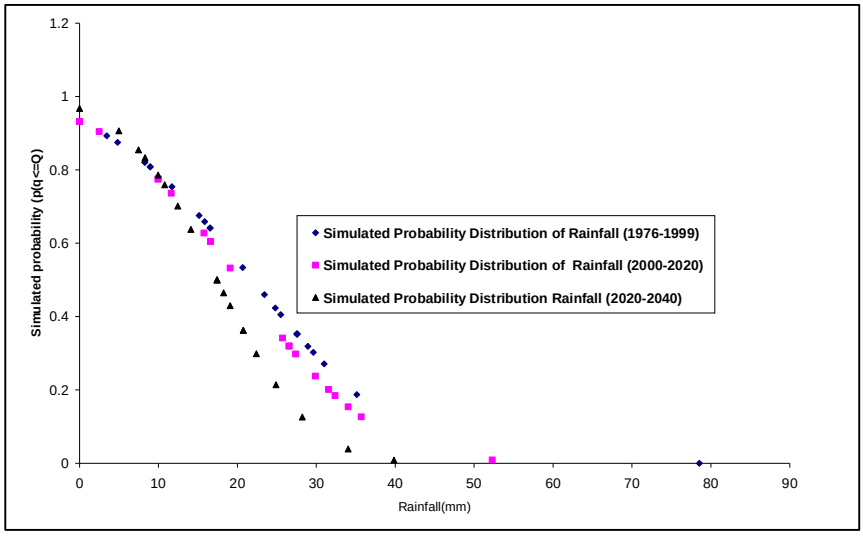

Fig. 8. Simulated probability distribution of rainfall for 1976-1999, 2000-2020 and 2020-2040

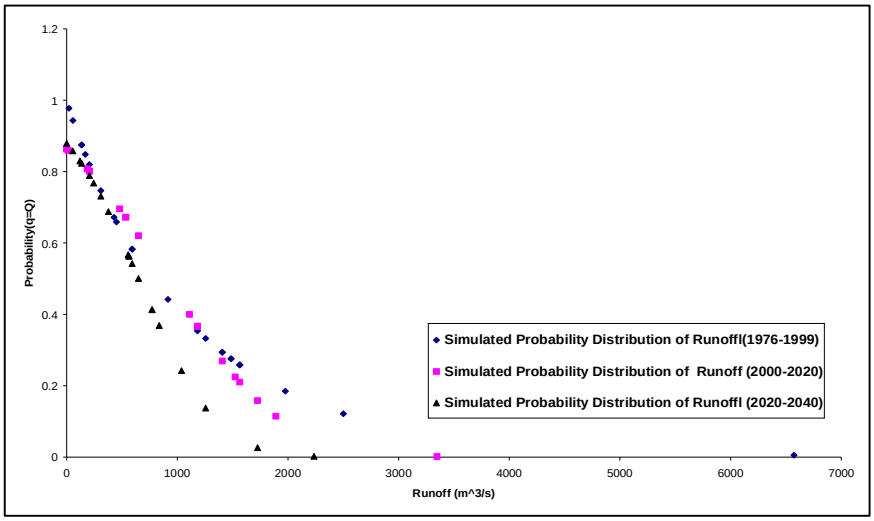

Fig. 9. Simulated probability distribution of flood (maximum runoff) for 1976-1999, 2000-2020 and 2020-40

Acknowledgments: This study was a part of a flood management project entitled "Flood plane zoning downstream of Kajoo and Kariani river basins and the design of a flood warning system" sponsored by the Sistan and Baloochestan Water Authority.

REFERENCES

1. Karamouz, M., Imani, M., Ahmadi, A. & Moridi, A. (2009). Optimal flood management options with probabilistic optimization: A case study. *Iranian Journal of Science & Technology, Transaction B: Engineering*, Vol. 33, No. B1, pp 109-121.
2. Arnell, N. W., Reynard, N., King, R., Proudhomme, C. & Branson, J. (1997). Effects of climate change on river flows and groundwater recharge: guidelines for resource assessment. Environment Agency Technical Report W82, Bristol.
3. Hansen, A. C., Liu, L., Linde, J. J., Mark, O. & Mikkelsen, P. S. (2005). Accounting for uncertainty in urban drainage system performance assessment using safety factors applied to runoff. *10th International Conference on Urban Drainage*, Copenhagen/Denmark.
4. Jiang, T., Chen, Y. D., Xu, C. Y., Chen, X. & Singh, V. P. (2007). Comparison of hydrological impacts of climate change simulated by six hydrological models in the Dongjiang Basin, South China. *Journal of Hydrology*, Vol. 336, pp. 316-333.
5. Burger, C. M., Kolditz, O., Fowler, H. J. & Blenkinsop, S. (2007). Future climate scenarios and rainfall-runoff modeling in the Upper Gallego catchment (Spain). *Elsevier, Journal of Environmental Pollution.*
6. Krysanova, V., Hattermann, F. & Wechsung, F. (2007). Implications of complexity and uncertainty for integrated modeling and impact assessment in river basins. *Journal of Environmental Modeling and Software*, Vol. 22, pp. 701-709.
7. Day, G. N. (1995). Extended streamflow forecasting using NWSRFS. *Journal of Water Resources Planning and Management*.
8. Ingram, J. J., Fread, D. L. & Larson, L. W. (1998). Improving real time hydrological service in the USA, PartI: Ensemble generated probabilistic forecast. *British Hydrological Society*.
9. Azmi, M., Araghinejad, S. & Kholghi, M. (2010). Multi model data fusion for hydrological forecasting using K-nearest neighbour method. *Iranian Journal of Science & Technology, Transaction B: Engineering*, Vol. 34, No. B1, pp 81-92.
10. Harpham, C. & Wilby, R. (2005). Multi-Site downscaling of heavy daily rainfall occurrence and amounts. *Journal of Hydrology*, Vol. 312, pp. 235-255.
11. Ekstrom, M., Hingray, B., Mezghani, A. & Jones, P. D. (2005). Regional climate model data used within the SWURVE project 2: addressing uncertainty in regional climate model data for five European case study areas. *Hydrology and Earth Systems Science* (in press).
12. Wilby, R. L., Dawson, C. W. & Barrow, E. M. (2002). SDSM- a decision support tool for the assessment of regional climate change impacts. *Journal of Environmental Modeling and Software*, Vol. 17, pp. 147–159.
13. Sajjad Khan, M., Coulibaly, P. & Dibike, Y. (2006). Uncertainty analysis of statistical downscaling methods. *Journal of Hydrology*, Vol. 319, pp. 357-382.
14. Conover, W. J. (1980). *Practical nonparametric statistics*. Second ed. Wiley, New York.
15. Neter, J., Wasserman, W. & Whitmore, G. A. (1978). *Applied statistics.* Allyn and Bacson, Inc., Massachusetts, USA.
16. Brown, M. B. & Forsythe, A. B. (1974). Robust tests for the equality of variances. Journal of American State Association, Vol. 69, pp. 364–367.
17. Karamouz, M. (2007). Flood plane zoning downstream of Kajoo and Kariani river basins and the design of flood warning system. *Sistan and Baloochestan Water Authority*.
18. Karamouz, M., Nazif, S., Fallahi, M. & Imen, S. (2007). Assessment of uncertainty in flood forecasting using downscaled rainfall data. *Proceedings of ASCE Environmental and Water Resources Institute Conference*, Tampa, Florida, USA.
19. Benjamin, J. R. & Cornell, C. A. (1970). *Probability, statistics, and decision for Civil engineers*. McGraw-Hill Book Company, New York.
20. Karamouz, M., Fallahi, M., Nazif, S. & Ahmadi, A. (2006). Flood forecasting using downscaled long- lead rainfall forecast. *The Second Korea-Iran Joint Workshop on Climate Modeling*, South Korea.